

## Fouling dynamics modelling in the ultrafiltration of PEGs

M. Cinta Vincent Vela<sup>a\*</sup>, Silvia Álvarez Blanco<sup>a</sup>, Jaime Lora García<sup>a</sup>,  
Enrique Bergantiños Rodríguez<sup>b</sup>

<sup>a</sup>Department of Chemical and Nuclear Engineering, Polytechnic University of Valencia,  
C/Camino de Vera s/n 46022 Valencia, Spain

Tel. +34 963877000; ext. 76381; Fax +34 963877639; email: mavinve@iqn.upv.es

<sup>b</sup>Department of Chemical Engineering, Polytechnical Institute José A. Echeverría,  
Ave. 114, No. 11901, Havana, Cuba

Received 14 December 2006; accepted 3 January 2007

---

### Abstract

The aim of this work was to compare the data on flux decline with time obtained with ultrafiltration experiments of polyethylene glycols (PEGs) performed under different experimental conditions (transmembrane pressures and crossflow velocities) and the theoretical predictions for these experimental conditions obtained with the model proposed by Ho and Zydney (2000). This model considers that two main fouling mechanisms, pore blocking and cake formation, can occur when macromolecules are ultrafiltered. In this work, flux decline predictions were achieved without using empirical parameters dependent on operating conditions. The fouling experiments were performed using monotubular ZrO<sub>2</sub>-TiO<sub>2</sub> ceramic membranes with a molecular weight cut off (MWCO) of 15 kDa (Orelis, France). A 5 g/L PEG (35,000 Da molecular weight) aqueous solution was used as feed. The model does not accurately describe the fouling dynamics under every experimental condition tested. However, the best predictions were obtained for high transmembrane pressures (TMPs) and low crossflow velocities when the cake layer is more likely to form.

*Keywords:* Flux decline; Fouling dynamics; Ultrafiltration; Macromolecules

---

### 1. Introduction

Crossflow ultrafiltration (UF) has been applied successfully in many industrial applications, such as concentration and purification of solutions and solvent extraction [1,2]. One of the major

drawbacks that limit the use of UF technology is fouling of the membranes [3]. Fouling consists in the deposition of feed components on the membrane surface or within the pores with the consequent decline in flux with time.

Modelling of ultrafiltration processes is essential to successfully design and operate ultrafiltration plants selecting the optimal operational

---

\*Corresponding author.

conditions to minimize fouling and maximize permeate production. The non-steady state nature of UF processes requires unsteady-state models to describe transport through the UF membranes. Many models for the description of the fouling phenomenon during ultrafiltration have been developed [4]. In practice mostly empirical or semi-empirical models have been used to explain flux decline with time [5]. Although they are very accurate, experimentation is required in order to apply them.

In this paper, predicted results of permeate flux decline with time by a model that considers two main fouling mechanisms: pore blocking and cake formation, were compared with experimental results. Flux decline predictions were achieved without using empirical parameters dependent on operating conditions.

## 2. Materials and methods

### 2.1. Materials

Polyethylene glycol (PEG) aqueous solution was used as feed. The PEG was supplied by Merck-Schuchardt (Germany) and had a molecular weight of 35,000 g/mol. To prepare the solutions for membrane cleaning, NaOH in pellets or flakes supplied by Panreac (Spain) was used.

Carbosep M2 monotubular ceramic membranes supplied by Orelis, S.A. (France) were used. These membranes consisted of a single cylindrical tube of 20 cm length, 10 mm external diameter and 6 mm internal diameter. The active layer consisted of a thin  $ZrO_2$ - $TiO_2$  layer deposited on the internal side of a carbon support. The membrane area was 35.5 cm<sup>2</sup> and the molecular weight cut off (MWCO) of the membrane was 15 kg/mol, which is equivalent to a pore diameter of approximately 4 nm.

### 2.2. Experimental rig

The experimental device used in the ultrafiltration experiments is described elsewhere [6].

To ensure a constant concentration in the feed tank several things were considered. The first one was that both the permeate and the retentate were recycled back to the feed tank. The second one was that due to the small membrane area and the big volume of the feed tank, the quantity of PEG deposited on the membrane was minimum compared to the total amount of PEG in the feed tank and it will not alter the feed tank concentration.

### 2.3. Theory

The dynamic model for crossflow ultrafiltration described here combines two fouling mechanisms: pore blocking and cake formation [7]. The model integrates these two phenomena in the same mathematical equation, Eq. (1), for the description of permeate flux decline.

$$J_p = \left\{ \begin{array}{l} \left[ 1 - \left( \exp \left( \frac{\alpha \cdot \Delta P \cdot C_0}{\mu \cdot R_m} \cdot t \right) \right)^{-1} \right] \frac{\Delta P \cdot R_m}{\mu \cdot R_m \cdot (R_m + R_g)} \\ + \left[ \exp \left( \frac{\alpha \cdot \Delta P \cdot C_0}{\mu \cdot R_m} \cdot t \right) \right]^{-1} \frac{\Delta P}{\mu \cdot R_m} \end{array} \right\} \quad (1)$$

In Eq. (1)  $J_p$  is the permeate flux,  $\alpha$  is the pore blocking parameter,  $\Delta P$  is the transmembrane pressure,  $C_0$  is the feed concentration,  $t$  is time,  $\mu$  is the dynamic viscosity of the permeate,  $R_m$  is the membrane hydraulic resistance and  $R_g$  is the specific resistance of the gel layer.

The first term in Eq. (1) controls permeate flux decline with time for long time scales and considers permeation across the partially blocked membrane pores.

For short time scales, permeate flux decline with time is controlled by the second term, which takes into account permeation across the open membrane pores. According to the second term, permeate flux decline with time is linear at the beginning of ultrafiltration process.

Several hypothesis were considered in the development of the model: total pore blocking is not achieved because there is always a little permeate flux through the blocked membrane pores, the gel layer only forms over the membrane surface in which membrane pores have been previously blocked, pore blocking and gel layer formation velocity are proportional to the convective flow of molecules towards the membrane and permeate flux through open membrane pores diminishes exponentially with time with a velocity proportional to the feed concentration.

In the Eq. (1), the pore blocking parameter is given by Eq. (2):

$$\alpha = \frac{f \cdot A_{\text{pore}}}{M_{\text{agg}}} \quad (2)$$

where  $A_{\text{pore}}$  is the single membrane pore area and  $M_{\text{agg}}$  is the weight of a solute molecule aggregate.

The specific resistance of the gel layer in Eq. (1) increases with time and it is calculated by means of Eq. (3)

$$R_g = (R_m + R_{co}) \times \sqrt{1 + \frac{2 \cdot f' \cdot a \cdot \Delta P \cdot C_0 \cdot t}{\mu \cdot (R_m + R_{co})^2}} - R_m \quad (3)$$

where  $R_{co}$  is the initial resistance of the gel layer,  $f'$  is the fractional amount of solute which contributes to the gel layer growth and  $a$  is the specific resistance of the cake layer. The specific resistance of the cake layer in Eq. (3) is defined in Eq. (4)

$$a = 45 \cdot \frac{(1-\varepsilon)}{\varepsilon^3 \cdot a_p^2 \cdot \rho_g} \quad \varepsilon = 1 - C_{gv} \quad (4)$$

where  $\varepsilon$  is the cake porosity,  $a_p$  is the radius of the solute molecule,  $\rho_g$  is the density of the gel

layer and  $C_{gv}$  is the gel layer concentration. For the calculation of the density and concentration of the gel layer, the equation proposed by Lee et al. was employed [8].

The Stokes–Einstein radius of PEG molecules as a function of the molecular weight (MW) was estimated by means of Eq. (5) [9]. All the variables in Eq. (5) are expressed in the international system of units (SI).

$$a_p = (0.262 \cdot (\text{MW})^{0.5} - 0.3) \cdot 10^{-10} \quad (5)$$

Eq. (5) is valid for a MW range of 200–40,000 Da and has been very often used [10,11].

The model has been applied in ultrafiltration processes with protein effluents [12,13] and with natural organic matter [14,15]. In all these cases model parameters were empirically estimated. However, the model parameters were theoretically calculated in this paper.

#### 2.4. Experimental procedure

The water permeability of the membrane at 25°C was determined with deionised water.

The feed solution was prepared by dissolving PEG in deionised water until a concentration of 5 g/L was achieved. The feed solution was not allowed to pass through the membrane until the temperature was stabilized at a value of 25°C. The pilot plant was stopped after 7 h of operation, time enough to reach quasi-steady-state conditions.

The experiments were performed at different feed flow rates and transmembrane pressures (TMPs). The flow rate was varied between 1 and 3 m/s and the TMP was varied between 0.1 and 0.4 MPa. All the runs were carried out at a temperature of 25°C. The same membrane was used for all the experiments. After each run the membrane was cleaned, and afterwards the water permeability of the membrane was checked.

The cleaning cycle of the membrane was the following. First the membrane was rinsed with

deionised water, then it was cleaned with an aqueous NaOH solution and finally it was rinsed again with deionised water. Once the cleaning process was finished, the water permeability of the membrane was measured and the initial permeability of the membrane was completely recovered after the cleaning cycle.

### 3. Results and discussion of the application to macromolecular ultrafiltration

The value of the membrane resistance obtained in the experiments performed with deionised water was  $6.897 \times 10^{12} \text{ m}^{-1}$ .

Experimental and predicted results are compared in Figs. 1–3. In Fig. 1, results correspond to a crossflow velocity of 1 m/s and four TMPs. The continuous lines correspond to the results predicted by the model and the symbols correspond to the experimental results. For long time scales permeate fluxes predicted by the model are inferior to those experimentally observed. However, the shape of the curve for permeate flux decline with time is similar for both experimental and predicted results.

Fig. 2 compares experimental and predicted permeate flux for a crossflow velocity of 2 m/s. The discrepancies between predicted and experimental data for long time scales were similar to the ones for the crossflow velocity of 1 m/s. In

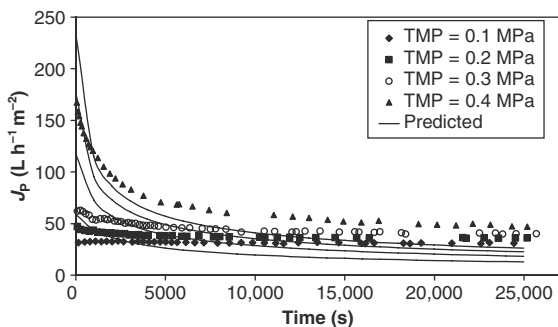


Fig. 1. Comparison between experimental (symbols) and predicted permeate flux (lines) at a crossflow velocity of 1 m/s.

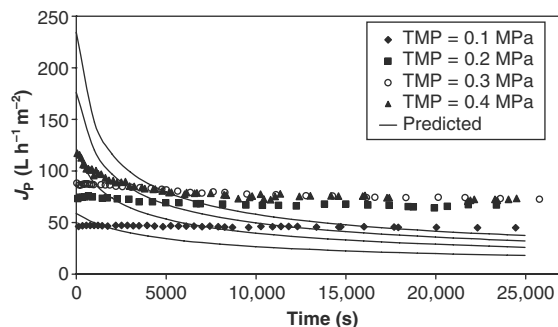


Fig. 2. Comparison between experimental (symbols) and predicted permeate flux (lines) at a crossflow velocity of 2 m/s.

this case, the shape of the curve for flux decline with time estimated by the model differs more from that experimentally observed than in the case of lower crossflow velocities. The model predicts a greater initial permeate flux decline than the experimental one. The reason for this may be that a crossflow velocity of 2 m/s could be too high for a cake layer to form. In addition, another fouling mechanism different from cake layer formation or pore blocking, that was not taken into account by the model, could take place. For short time scales, predicted permeate fluxes were higher than the experimental ones and the model predicted lower fouling than that experimentally observed.

Fig. 3 compares experimental and predicted permeate flux for a crossflow velocity of 3 m/s. As well as for a crossflow velocity of 2 m/s, the discrepancies between predicted and experimental data for long time scales were similar to the ones obtained for a crossflow velocity of 1 m/s. However, for short time scales the model predicts lower fouling than that experimentally observed. In this case, as well as for a crossflow velocity of 2 m/s, the shape of the curve for permeate flux decline with time estimated by the model differs more from that experimentally observed than in the case of lower crossflow velocities (1 m/s). Experimentally observed permeate flux decline with time was small while predicted permeate flux decline with time was much higher. This

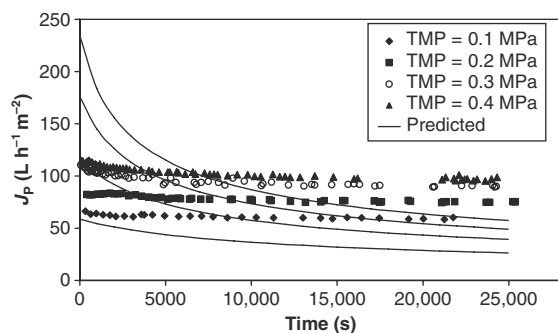


Fig. 3. Comparison between experimental (symbols) and predicted permeate flux (lines) at a crossflow velocity of 3 m/s.

discrepancy between model predictions and experimental results may be due to the fact that the main fouling mechanism is not cake formation and/or pore blocking for this crossflow velocity.

For all the crossflow velocities, the model accounts the effect on permeate flux caused by an increase on TMP that implies a transition from a pressure controlled process to a mass transfer controlled process. Moreover, as TMP increases, permeate fluxes at different TMPs are more similar. The model considers that at the beginning of an ultrafiltration process permeate flux decline is a consequence of the pore blocking phenomenon. For this reason, an exponential decrease in permeate flux with time for low time scales can be observed in the results predicted by the model. Nevertheless, for high crossflow velocities and low tmPs no pore blocking phenomenon may occur under the experimental conditions tested because the permeate flux experimentally determined does not decrease exponentially with time.

#### 4. Conclusions

The model does not accurately describe the fouling dynamics under the experimental conditions tested. However, the lowest discrepancies between experimental results and those predicted

by the model were obtained for the experimental conditions that favour the formation of a cake layer: high TMPs and low crossflow velocities.

A comparison of the predicted values and the experimental ones shows that predictions are not good enough for any experimental condition tested. The inexistence of the pore blocking phenomenon under certain experimental conditions and the possibility of gel layer formation occurring for very short time scales may be the reason for the discrepancies between predicted and experimental results. In this way, these discrepancies could also be due to model hypothesis that may not be correct for the experimental conditions tested in this paper. For example, some of the membrane pores could be totally blocked. Moreover, the gel layer could form all over the membrane surface and not only over the membrane surface whose pores have been previously blocked.

#### Acknowledgement

The authors of this work wish to gratefully acknowledge the financial support of the Spanish Ministry of Science and Technology (MCYT) through its project no. CTQ2005-03398.

#### Symbols

$a$	specific resistance of the cake layer (m/kg)
$A_{\text{pore}}$	single membrane pore area (m <sup>2</sup> )
$a_p$	radius of the PEG molecule (m)
$C_{\text{gv}}$	gel concentration (v/v)
$C_0$	feed concentration (kg/m <sup>3</sup> )
$f'$	fractional amount of solute which contributes to the gel layer growth (dimensionless)
$J_p$	permeate flux (m/s)
$M_{\text{agg}}$	weight of a solute molecule aggregate (kg/aggregate)
$\Delta P$	transmembrane pressure (Pa)
$R_{c_0}$	initial resistance of the gel layer (m <sup>-1</sup> )

$R_g$	specific resistance of the gel layer ( $m^{-1}$ )
$R_m$	membrane hydraulic resistance ( $m^{-1}$ )
$t$	time (s)

### Greek letters

$\alpha$	pore blocking parameter defined in Eq. (2) ( $m^2/kg$ )
$\varepsilon$	cake porosity (dimensionless)
$\mu$	dynamic viscosity (kg/m/s)
$\rho_g$	density of the gel layer ( $kg/m^3$ )

### Abbreviations

MW	molecular weight
MWCO	molecular weight cut off
PEG	polyethylene glycol
SI	international system for units
TMP	transmembrane pressure
UF	ultrafiltration

### References

- [1] M.Z. Sulaiman, N.M. Sulaiman and B. Abdellah, Prediction of dynamic permeate flux during cross-flow ultrafiltration of polyethylene glycol using concentration polarization-gel layer model, *J. Membr. Sci.*, 189 (2001) 151–165.
- [2] M. Cheryan (Ed.), *Ultrafiltration and microfiltration handbook*, 2nd edn., CRC Press, New York, 1998.
- [3] A. Guadix, E. Sorensen, L.G. Papageorgiou and E.M. Guadix, Optimal design and operation of continuous ultrafiltration plants, *J. Membr. Sci.*, 235 (2004) 131–138.
- [4] E. Iritani, Y. Mukai and E. Hagihara, Measurements and evaluation of concentration distributions in filter cake formed in dead-end ultrafiltration of protein solutions, *Chem. Eng. Sci.*, 57 (2002) 53–62.
- [5] V. Gekas, P. Aimar, J.-P. Lafaille and V. Sánchez, A simulation study of the adsorption — concentration polarisation interplay in protein ultrafiltration, *Chem. Eng. Sci.*, 48 (1993) 2753–2765.
- [6] M.C. Vincent Vela, S. Álvarez Blanco and J. Lora García, Crossflow ultrafiltration of cake forming solutes: a non-steady state model, *Desalination*, 184 (2005) 347–356.
- [7] C.-C. Ho and A.L. Zydney, A combined pore blockage and cake filtration model for protein fouling during microfiltration, *J. Colloid Interf. Sci.*, 232 (2000) 389–399.
- [8] S. Lee, J. Kim and C.H. Lee, Analysis of  $CaSO_4$  scale formation mechanism in various nanofiltration modules, *J. Membr. Sci.*, 163 (1999) 63–74.
- [9] C. Tam and A. Trembley, Membrane pore characterization — comparison between single and multicomponent solute probe techniques, *J. Membr. Sci.*, 57 (1991) 271–287.
- [10] P. Puhlfürß, A. Voigt, R. Weber and M. Morbe, Microporous  $TiO_2$  membranes with a cut off <500 Da, *J. Membr. Sci.*, 174 (2000) 123–133.
- [11] D. Möckel, E. Staude and M.D. Guiver, Static protein adsorption, ultrafiltration behavior and cleanability of hydrophilized polysulfone membranes, *J. Membr. Sci.*, 158 (1999) 63–75.
- [12] A.L. Zydney and C.-C. Ho, Scale-up of microfiltration systems: fouling phenomena and  $V_{max}$  analysis, *Desalination*, 146 (2002) 75–81.
- [13] L. Palacio, C.-C. Ho, P. Prádanos, A. Hernández and A.L. Zydney, Fouling with protein mixtures in microfiltration: BSA–lysozyme and BSA–pepsin, *J. Membr. Sci.*, 222 (2003) 41–51.
- [14] W. Yuan, A. Kocic and A.L. Zydney, Analysis of humic acid fouling during microfiltration using a pore blockage–cake filtration model, *J. Membr. Sci.*, 198 (2002) 51–62.
- [15] M. Taniguchi, J.E. Kilduff and G. Belfort, Modes of natural organic matter fouling during ultrafiltration, *Environ. Sci. Technol.*, 37 (2003) 1676–1683.